AFWL-TR-
88-106

(2)

DETONATION CHARACTERISTICS OF MIXTURES OF HMX AND EMULSION EXPLOSIVES

J. Renick
J. Sanchez

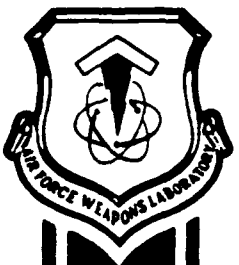

April 1989

Final Report

A F W L

Approved for public release; distribution unlimited.

AIR FORCE WEAPONS LABORATORY
Air Force Systems Command
Kirtland Air Force Base, NM 87117-6008

This final report was prepared by the Air Force Weapons Laboratory, Kirtland Air Force Base, New Mexico, Job Order 672A0733. Lieutenant Mike Turnipseed (NTED) was the Laboratory Project Officer-in-Charge.

When Government drawings, specifications, or other data are used for any purpose other than in connection with a definitely Government-related procurement, the United States Government incurs no responsibility or any obligation whatsoever. The fact that the Government may have formulated or in any way supplied the said drawings, specifications, or other data, is not to be regarded by implication, or otherwise in any manner construed, as licensing the holder, or any other person or corporation; or as conveying any rights or permission to manufacture, use, or sell any patented invention that may in any way be related thereto.

This report has been authored by employees of the United States Government. Accordingly, the United States Government retains a nonexclusive, royalty-free license to publish or reproduce the material contained herein, or allow others to do so, for the United States Government purposes.

This report has been reviewed by the Public Affairs Office and is releasable to the National Technical Information Service (NTIS). At NTIS, it will be available to the general public, including foreign nationals.

If your address has changed, if you wish to be removed from our mailing list, or if your organization no longer employs the addressee, please notify AFWL/NTED, Kirtland AFB, NM 87117-6008 to help us maintain a current mailing list.

This report has been reviewed and is approved for publication.

Mike Turnipseed

MIKE TURNIPSEED
Lieutenant, USAF
Project Officer

FOR THE COMMANDER

Laddie L. Marin, Jr.

LADDIE MARIN, JR.
Major, USAF
Chief, Technology Branch

Carl L. Davidson

CARL L. DAVIDSON
Colonel, USAF
Chief, Civil Engrg Research Division

DO NOT RETURN COPIES OF THIS REPORT UNLESS CONTRACTUAL OBLIGATIONS OR NOTICE ON A SPECIFIC DOCUMENT REQUIRES THAT IT BE RETURNED.

UNCLASSIFIED
SECURITY CLASSIFICATION OF THIS PAGE

REPORT DOCUMENTATION PAGE

Form Approved
OMB No 0704-0188

1a. REPORT SECURITY CLASSIFICATION Unclassified	1b. RESTRICTIVE MARKINGS
2a. SECURITY CLASSIFICATION AUTHORITY	3. DISTRIBUTION/AVAILABILITY OF REPORT Approved for public release; distribution unlimited.
2b. DECLASSIFICATION/DOWNGRADING SCHEDULE	
4. PERFORMING ORGANIZATION REPORT NUMBER(S) AFWL-TR-88-106	5. MONITORING ORGANIZATION REPORT NUMBER(S)
6a. NAME OF PERFORMING ORGANIZATION Air Force Weapons Laboratory 6b. OFFICE SYMBOL (If applicable) NTED	7a. NAME OF MONITORING ORGANIZATION
6c. ADDRESS (City, State, and ZIP Code) Kirtland Air Force Base, New Mexico 87117-6008	7b. ADDRESS (City, State, and ZIP Code)
8a. NAME OF FUNDING/SPONSORING ORGANIZATION Ballistic Missile Office 8b. OFFICE SYMBOL (If applicable)	9. PROCUREMENT INSTRUMENT IDENTIFICATION NUMBER
8c. ADDRESS (City, State, and ZIP Code) Norton AFB, California 92409-6468	10. SOURCE OF FUNDING NUMBERS PROGRAM ELEMENT NO. 64312F; PROJECT NO 672A; TASK NO 07; WORK UNIT ACCESSION NO 33

11. TITLE (Include Security Classification)
DETONATION CHARACTERISTICS OF MIXTURES OF HMX AND EMULSION EXPLOSIVES

12. PERSONAL AUTHOR(S)
[illegible]h Renick and John Sanchez

13a. TYPE OF REPORT	13b. TIME COVERED	14. DATE OF REPORT (Year, Month, Day)	15. PAGE COUNT
Final	FROM Mar 87 TO Dec 87	1989, April	66

16. SUPPLEMENTARY NOTATION
This research was funded by the Ballistic Missile Office, Norton AFB, CA 92409-6468.

17. COSATI CODES			18. SUBJECT TERMS (Continue on reverse if necessary and identify by block number)
FIELD	GROUP	SUB-GROUP	
19	01		Explosives; Ammonium Nitrate;
07	04		Emulsion Explosives;
			Composite Explosives;

19. ABSTRACT (Continue on reverse if necessary and identify by block number)

The detonation characteristics of various mixtures of HMX and an aqueous emulsion explosive have been determined. The emulsion explosive consisted of ammonium-nitrate, sodium-nitrate and water in the dispersed phase, and an emulsifier/oil mixture in the continuous phase. The HMX/emulsion mixtures of from 10 to 50 percent HMX were prepared and evaluated in cylindrical and conical charge experiments. Insufficient data were collected to provide a comprehensive description of the detonation behavior of HMX/emulsion explosives over the entire range of possible mixtures; however, it was possible to provide a definitive description of the velocity-mixture-diameter relationships over the range of 20 to 50 percent HMX and a qualitative description elsewhere. Keywords:

(over)

20. DISTRIBUTION/AVAILABILITY OF ABSTRACT	21. ABSTRACT SECURITY CLASSIFICATION
☒ UNCLASSIFIED/UNLIMITED ☐ SAME AS RPT ☐ DTIC USERS	Unclassified
22a. NAME OF RESPONSIBLE INDIVIDUAL Mike Turnipseed	22b. TELEPHONE (Include Area Code) (505) 846-6483
	22c. OFFICE SYMBOL AFWL/NTED

DD Form 1473, JUN 86 Previous editions are obsolete.

SECURITY CLASSIFICATION OF THIS PAGE
UNCLASSIFIED

19. ABSTRACT (continued)

The important results of this research are summarized as follows:

(1) At a given diameter, an increase in HMX loading results in an increase in detonation velocity. As HMX loading increases, the failure diameter decreases and the detonation velocity at failure increases.

(2) The effect of diameter on detonation velocity for HMX/emulsion explosive mixtures is adequately described by the Campbell-Engelke model. This is clearly demonstrated in the 50/50 mixture and the trend of downward concavity in plots of detonation velocity versus inverse charge diameter for other mixtures was observed.

(3) Addition of approximately 20 percent HMX to an emulsion explosive results in a substantial increase in initiation sensitivity. This observation is based on the premise of an inverse relationship between failure diameter and initiation sensitivity for the HMX/emulsion explosive system.

ACKNOWLEDGEMENTS

This research was conducted at the Center for Explosives Technology Research, New Mexico Institute of Mining and Technology, Socorro, NM under the guidance and supervision of Dr. Per-Anders Persson. His patient guidance and many helpful discussions are appreciated.

The New Mexico Engineering Research Institute, University of New Mexico sponsored this effort with funding from the Air Force Weapcns Laboratory, Kirtland AFB, NM. Mr. Ken Bell was the project officer in charge.

Special thanks to Jamin Lee, Fred Sandstrom, Jimmie Oxley, Scott Sullivan, Tom Gould and Phil Anthony for their support in conduct of this program. The many hours of discussion and assistance were very enjoyable as well as rewarding.

We are especially grateful to Lisa Olver for her support in the preparation of emulsions and test articles. Her quest for "a better way" will not soon be forgotten.

M-1 Division at Los Alamos National Laboratories (LANL) provided HMX/emulsion hazards testing and mixture preparations. Without the LANL support this research would not have been possible.

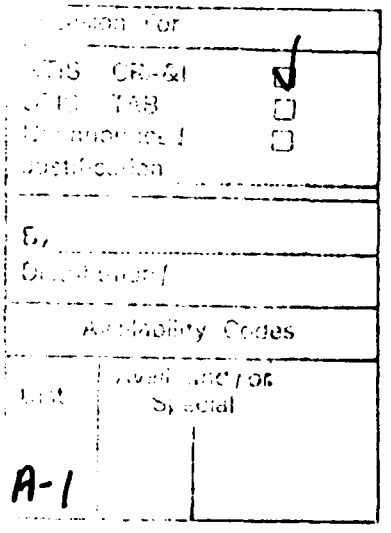

TABLE OF CONTENTS

LIST OF FIGURES

LIST OF TABLES

SECTION 1
INTRODUCTION

BACKGROUND

Since the signing of the Limited Test-Ban Treaty in 1963 which prohibited testing of nuclear weapons in the atmosphere, it has been necessary to test the survivability, vulnerability and hardness of military systems to nuclear weapons blast and shock effects through simulation methods using conventional high explosives. Since the mid-1960s, researchers have successfully adapted both military and commercial explosives to the problems of nuclear weapons effects (NWE) simulation. After 25 years of testing, a wide variety of experiments have been conducted using quantities of explosives ranging from a few kilograms to several million kilograms. As the sophistication of experiments increased, the performance and characterization of the explosives used in these experiments became of greater importance, expecially with the development of large finite difference hydrodynamic codes used to design, predict and analyze major test events. The trend in recent years has been toward larger scale tests in which the explosive cost is an important consideration.

The development of emulsion explosives technology in the past 20 years in the U. S. has had a strong impact on the commercial explosives industry and their main customer, the mining industry. Only in recent years has serious consideration been given to military applications of emulsions. With the wide variety of emulsion formulations available, the variety of possible additives (molecular explosives, powdered metals, oxidizers, etc.) and the control over density (microballoons) and mechanical properties (formulation and processing), a wide range of detonation and mechanical properties appear to be potentially available.

Of particular interest to the NWE technical community is the use of emulsions that can be cast to form rigid charges in a variety of shapes. For instance, there is current interest in the use of very energetic explosives in small spherical charge experiments (500 kg) and in the use

of less energetic (and less expensive) explosives in large spherical charge experiments (500,000 kg), both for height-of-burst experiments. The issues of safety, thermal stability, initiation sensitivity, detonation performance, mechanical properties, processing methods, handling and transportation, environmental durability and cost are all important.

Emulsion explosives exhibit certain inherent advantages over other commercial explosives such as ammonium nitrate/fuel oil (ANFO) and slurries, both of which have been used extensively by the NWE community. These advantages are a result of the physical and chemical nature of the emulsion structure. The salt solution (oxidizer) is discontinous and is dispersed as small cells (less than 10 μm diameter) throughout the fuel. This results in very good intimacy of mixing between the fuel and oxidizer, which in turn results in a matrix with a high density and high detonation velocity relative to ANFO. In addition, the water-soluble salt solution is isolated from moisture by the thin fuel film resulting in a water-resistant matrix.

Emulsions are classed as heterogeneous with respect to their initiation behavior in response to mechanical shock. Campbell, et al[1,2] showed in a classic set of experiments that homogeneous explosives (such as liquid nitromethane) and heterogeneous explosives (solid molecular explosives, slurries, emulsions, etc.) behave in fundamentally different ways during initiation. In homogeneous explosives initiation occurs due to thermal effects caused by shock compression. After the initiating shock has propagated a short distance into the explosive, initiation occurs at the explosive surface where the shock was initially applied and a detonation front develops. The detonation front rapidly overtakes the shock, after which, steady detonation occurs. In the case of a heterogeneous explosive, initiation occurs due to the presense of hot spots and the detonation front develops immediately behind the shock. Generally, an overshoot in detonation velocity occurs in heterogeneous explosives when initiated by strong shocks; but, after the detonation front has propagated for some distance, the steady-state detonation

velocity is achieved. Generally, a much more intense shock is required to initiate homogeneous explosives than heterogeneous explosives.

Due to the inherent insensitivity of most emulsion formulations, it is necessary to increase their initiation sensitivity by the use of additives. The additives can be either high density inert particles, energetic particles (with an initiation sensitivity greater than that of the emulsion) or voids. In each case, it is believed that localized regions of very high energy density (hot spots) are produced resulting in high chemical reaction rates which lead to thermal initiation. In the case of high density particles, the increased energy density is due to shock interactions caused by the impedance mismatch between the particles and emulsion resulting in pressure induced hot spots. In the case of energetic particles, it is likely that shock interaction effects combine with the effects of particle initiation to generate initiation in the emulsion. In the case of voids, the increased energy density is due to hydrodynamic collapse. Johansson and Persson[3] provide a good review of the mechanisms believed to be involved in the hot spot model of initiation.

Lee[4] conducted an extensive investigation of the effects of microballoon size and loading on the detonation properties of emulsion explosives. His research was preceded by that of Yoshida, et al[5], and Hattori, et al[6]. The main results of Lee's work are summarized as follows: (1) At a given diameter, as the emulsion/microballoon density increases, the detonation velocity also increases until a maximum is reached, after which, the velocity begins to decrease until detonation failure occurs; (2) Failure diameter increases as the density increases; (3) At a given diameter, detonation velocity increases as the diameter of the microballoons decreases; and (4) Sensitivity to shock initiation increases as the density decreases.

Lee's results for unsieved microballoons are summarized in a <u>qualitative</u> manner in Figure 1 where detonation velocity, normalized to the infinite diameter detonation velocity of the pure emulsion (D/D_i), is plotted as a function of density, normalized to the pure emulsion

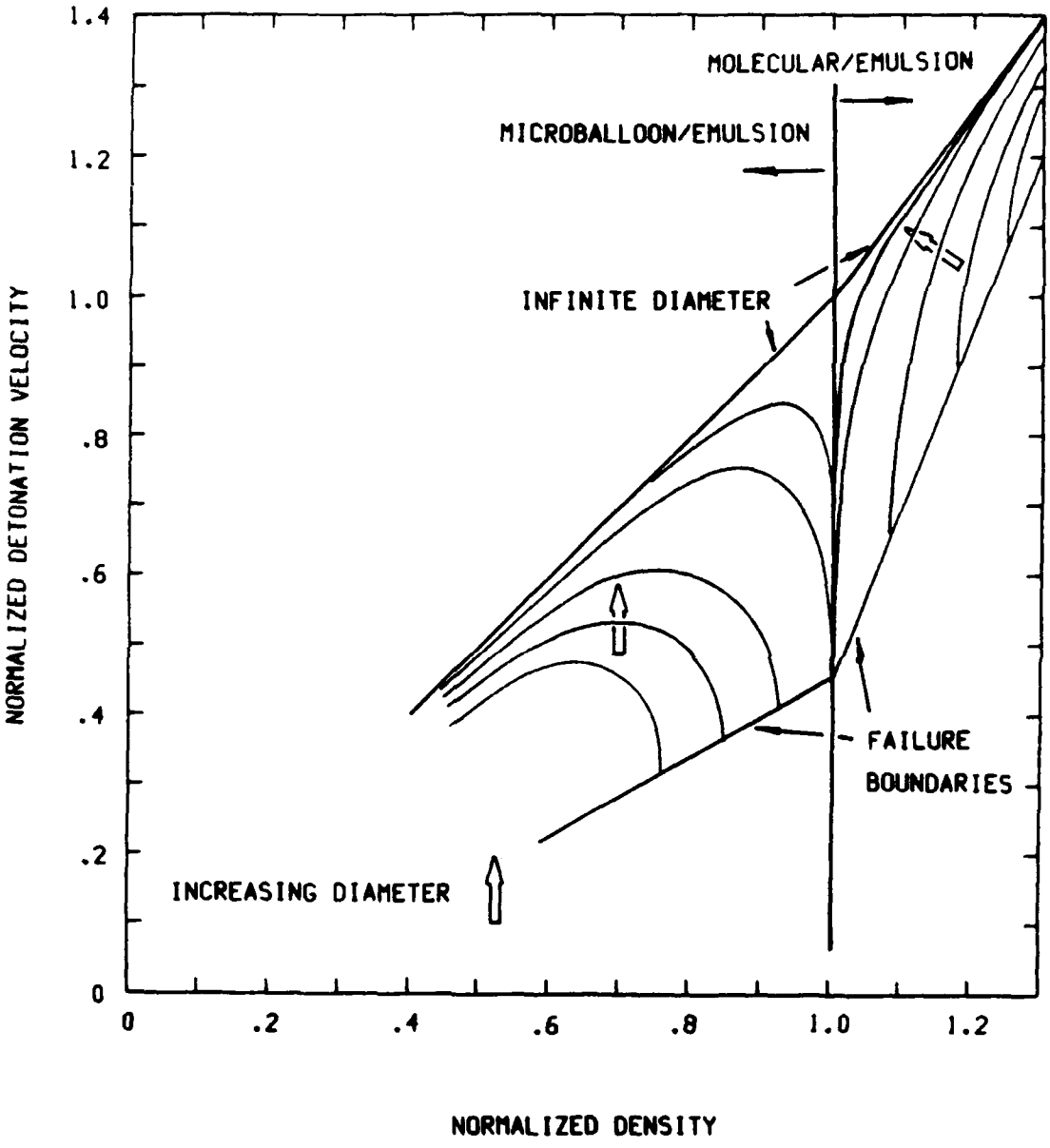

Figure 1. Detonation velocity as a function of density for emulsion/microballoon and molecular/emulsion explosive systems, normalized parameters.

density (ρ/ρ_0). Thus, the region to the left of ρ/ρ_0=1 is for emulsion/microballoon mixtures. The effects of explosive density and diameter on detonation velocity and failure diameter are revealed. In reality, the detonation velocity at failure for a given diameter is difficult to define experimentally and large uncertainties exist. The failure boundary in Figure 1 is thus to be taken as highly idealized, but nevertheless, descriptive of the qualitative behavior. The results of Becker-Kistiakowsky-Wilson (BKW) calculations are also shown to provide an idealized prediction of detonation velocity for an infinite diameter charge. Note that the behavior shown in Figure 1 is descriptive of (1) and (2) in the previous paragraph.

If a particulate molecular explosive was added to the pure emulsion then an extension of the results in Figure 1 could be made into the region where ρ/ρ_0>1, assuming that the density of the molecular explosive is greater than that of the pure emulsion. In this case, the detonation velocity at infinite diameter is expected to increase as the density of the mixture increases with the maximum obtained when the mixture reaches the limit of 100 percent molecular explosive. If the failure diameter and velocity at failure of the molecular explosive is known, then it is possible to construct a qualitative prediction of the effects of molecular/emulsion explosive density and charge diameter on detonation velocity and failure diameter. This qualitative prediction is shown in Figure 1 where the nominal values of octahydro-1,3,5,7-tetranitro-1,3,5,7-tetrazocine (HMX) density and detonation velocity have been assumed for the molecular explosive. Note that at a given charge diameter, the path of constant charge diameter through D/D_i vs ρ/ρ_0 space is continous if mixtures of all three components (microballoons, emulsion, molecular) are not considered and only diameters greater than the failure diameter of the pure emulsion are allowed. If diameters less than that of the failure diameter of the pure emulsion are allowed, then it is observed that the lines of constant diameter are discontinous, being "cut off" by the detonation failure boundaries. Note again that the purpose of Figure 1 is to represent only the qualitative behavior of the microballoon/emulsion and molecular/emulsion mixtures.

It would be a monumental task to conduct an experimental program in which the entire three-component (microballoon/emulsion/molecular) system was characterized. In addition, it is not clear that there would be applications where the detonation characteristics resulting from a particular mixture of all three components would be of interest. Regardless, the portions of the system represented in Figure 1 (microballoon/emulsion and molecular/emulsion mixtures) are of obvious interest and a complete characterization is warranted. Thus, it is the objective of this research program to investigate the detonation characteristics of a molecular/emulsion explosive system.

OBJECTIVE

The objective of this research is to characterize the detonation performance of molecular/emulsion explosive mixtures. Specifically, this research will generate the following experimental data: (1) detonation velocity as a function of molecular explosive loading and charge diameter; and (2) failure diameter and detonation velocity at failure as a function of molecular explosive loading. These results will be used to verify the qualitative predictions shown on the right side of Figure 1.

APPROACH

HMX was selected as the molecular explosive to be used in this research program. This selection was made for two reasons. First, a very energetic, well-characterized molecule was required. HMX clearly satisfies this requirement. Second, the Air Force Weapons Laboratory (AFWL) had HMX available to support this program. Since the time for this research was restricted, material availability was an important consideration.

The emulsion used in this program was prepared at the Center for Explosive Technology Research (CETR), New Mexico Institute of Mining and Technology (NM Tech); however, HMX/emulsion mixing was performed at the Los Alamos National Laboratory (LANL). This was necessary because the

materials processing laboratory construction at CETR had not progressed to the point that HMX drying and mixing could be performed. All experimental work was performed at the CETR Eagle Site located west of the NM Tech campus.

SECTION 2
EXPERIMENT DESCRIPTION

The primary data collected were from cylindrical and conical charge experiments. Charges were prepared by filling high-density urethane foam charge containers with the HMX/emulsion mixes. Detonation front position-time data were obtained with ionization pins, shorting pins and streak camera. In this section, test articles, HMX/emulsion preparation procedures, test article loading procedures and instrumentation systems are described.

CHARGE DESIGNS

Cylindrical Charges. Rigid high-density closed-cell urethane foam provided by General Plastics Inc., Tacoma, WA, was selected for use in fabrication of the cylindrical charge containers. This material is available at several densities. A density of 0.24 g/ml was chosen as a compromise between minimum cell size (high density) and minimum confinement (low density). A small cell size is desirable to provide a smooth machined surface. This material is machined easily with either wood or metal cutting techniques.

The cylindrical charge containers were designed to provide a run-up length of 10 diameters prior to the first time-of-arrival (TOA) pin. Four TOA pins were used in each charge with a spacing between pins equal to one charge diameter or 20 mm, whichever was greatest. The minimum spacing of 20 mm was imposed to insure that the combined effects of uncertainties in pin spacing (0.05 mm) and instrumentation sample rate (100 MHz) would always provide less than 0.5% uncertainty in the detonation velocity calculated from the TOA data. The pins were oriented normal to the charge axis and protruded a maximum of approximately 1 mm into the charge to minimize perturbations to the detonation front. Even though some curvature to the detonation front is known to be present, for steady-state detonation the velocities at the center of the charge and at its outer radius are identical.

For the limited nature of this research program, cylindrical charge containers for only five diameters were fabricated. Table 1 and Figure 2 summarize the important design features of the cylindrical charge containers. Each container was fabricated in two segments, as indicated in Figure 2, to facilitate machining and to maintain dimensional tolerances on the bore. For the two smallest charges the surfaces of the bores were sealed with paraffin to insure a smooth explosive-urethane interface. This was felt to be necessary for the smaller bores where the urethane cell size was on the order of 2% of the bore diameter.

As shown in Figure 2(b), small 1.6-mm-diameter acrylic rods were placed in the sides of the 3.18- and 6.35-mm-diameter charge containers to provide for light transmission in streak camera experiments. This technique was used for the smaller charges to avoid perturbation of the detonation front by the protrusion of the ionization pins into the bore. The acrylic rods were positioned flush with the bore.

Additional cylindrical charges were prepared for plate dent experiments. These consisted of cardboard and PVC pipe containers positioned on the center of steel plates. No TOA measurements were made in the plate dent experiments.

Conical Charges. The conical charges were fabricated through a cast operation using 0.08 g/ml urethane foam. General Plastics Inc. fabricated the molds and performed the casting operations. Four sections of different sizes were fabricated. Detailed descriptions of the sections and their dimensions are provided in Figure 3 and Table 1. The different size sections permitted selection of combinations which would bracket the expected failure diameter for any given HMX/emulsion mixture. Because the urethane forms a continous skin at the mold boundaries, the cast procedure resulted in a conical charge container with a mirror-smooth, precision surface. The sections were assembled by aligning them with a short tapered plug sized to fit the mating ends.

Table 1. Test article dimensions.[a]

TEST ARTICLE	L(mm)[b]	d(mm)	VOL(ml)	X1(m)	X(m)	C(m)
CYLINDER	355.6 x 2	51.50 +/- .15	1481.0	510	51	76
CYLINDER	177.8 x 2	26.10 +/- .18	190.0	260	26	51
CYLINDER	101.6 x 2	12.55 +/- .08	25.1	130	20	26
CYLINDER	63.5 x 2	6.35 +/- .06	4.0	60	20	13
CYLINDER	46.0 x 2	3.18 +/- .06	.7	28	20	10
CONE I	485.0	50.8 - 25.4	573.4	---	--	101.6
CONE II	243.0	25.4 - 12.7	71.8	---	--	101.6
CONE III	121.5	12.7 - 6.35	8.98	---	--	50.8
CONE IV	60.5	6.35 - 3.18	1.12	---	--	50.8

(a) Nominal Values. See Figures 2 and 3 for nomenclature.
(b) ± 0.25 mm

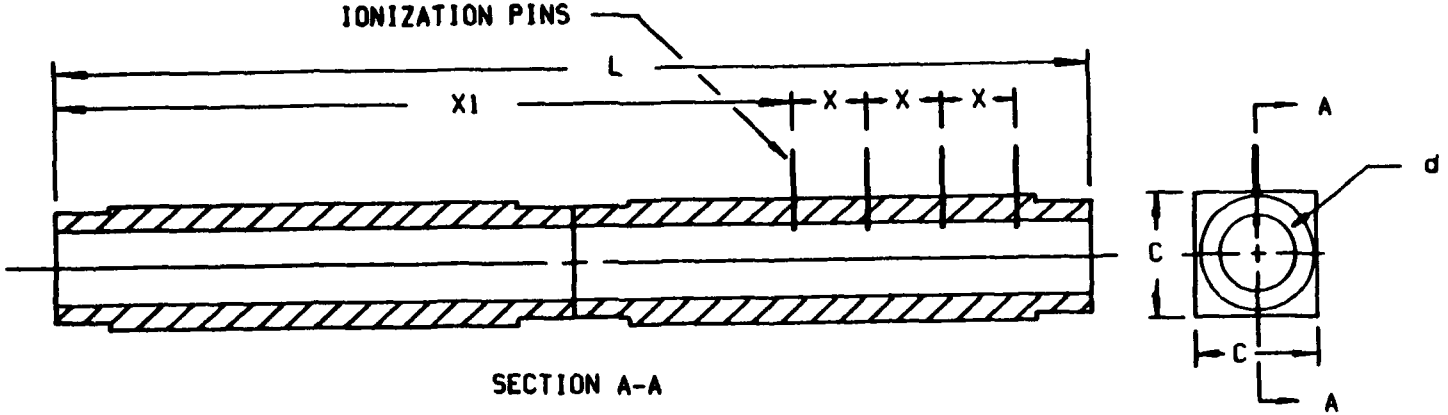

(a) PIN CONFIGURATION

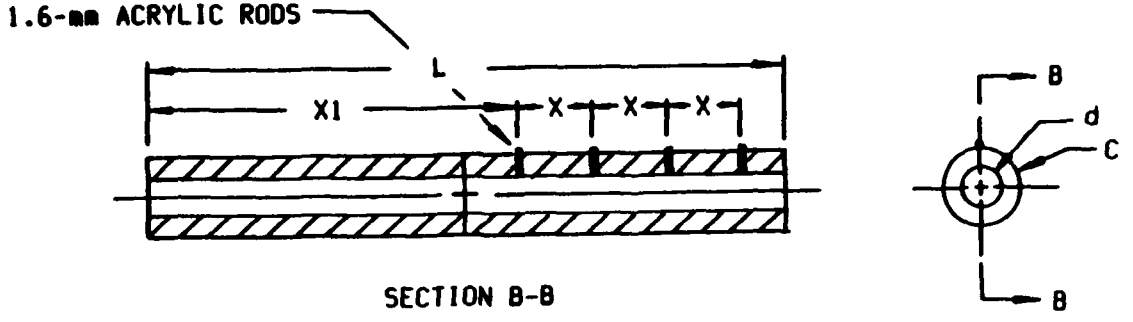

(b) STREAK CAMERA CONFIGURATION

Figure 2. Cylindrical charge container.

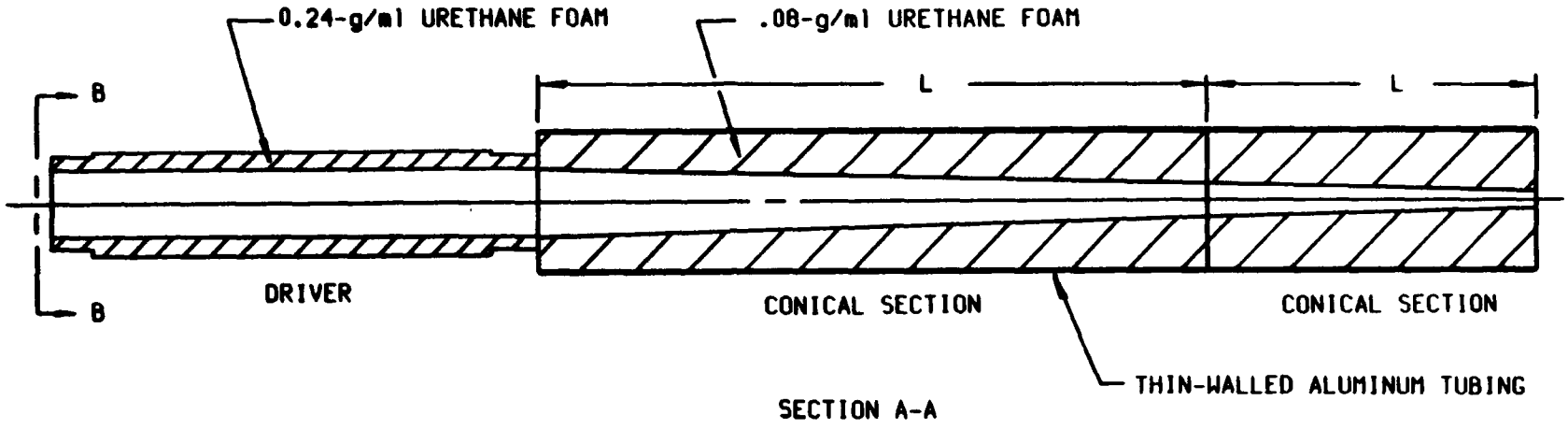

SECTION A-A

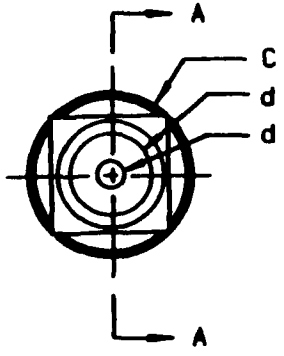

VIEW B-B

Figure 3. Conical charge container.

Note in Figure 3 that a single segment of a cylindrical charge container is attached to the large end of the conical charge container to serve as a driver stage to insure that the detonation front is near steady-state conditions as it enters the conical section. Shock position-time data was measured using a resistance probe positioned along the centerline of the charge for the section I-II conical charges (diameter from 50.8 to 12.7 mm). The two smaller conical charges assembled from sections II-III and III-IV were configured for streak camera measurements to avoid what was felt would be excessive perturbation by the resistance probe. This was accomplished by machining a narrow slot along the length of the conical sections and inserting an acrylic strip flush with the conical (interior) surface. The acrylic strip served to provide immediate quenching of the detonation light to provide a well-defined image of the detonation front trajectory. The camera viewing slot was 1.6 mm wide and aligned along the center of the acrylic strip.

HMX/EMULSION PREPARATION

Emulsion Preparation. The emulsion formulation selected was as follows:

Salt Solution	Ammonium Nitrate (AN)	71.5%
	Sodium Nitrate (SN)	10.0%
	Distilled Water	12.0%
Fuel	Light Mineral Oil/Emulsifier	6.5%

The salt solution (discontinous phase) is dispersed as tiny spherical cells of from 1- to 10-μm diameter throughout the fuel (continuous phase). The fuel consists of 2.7 parts light mineral oil to one part emulsifier.

The fuel was prepared by adding the emulsifier components to the light mineral oil at a temperature of 80 ^{0}C and stirring for 4 h. The emulsifier components consisted of 100 parts of polyisobutenyl succinic

anhydride (PSA) and 5.62 parts of a 50/50 mixture of diethanolamine and monoethanolamine. This formulation was developed based on discussions with Griffith and Oxley[7].

The emulsion was prepared as follows. The salt solution components were mixed together cold and then heated to 107 °C. Complete melting (as indicated by a clear solution) occurred at 82 °C. The fuel was heated in an oil bath to 107 °C and then placed in a preheated stainless steel thermally insulated mixing bowl (Kitchen Aid). The salt solution was added to the fuel (all at once) and mixed at a moderate speed (#4) for 3 min by a Kitchen Aid blender using a wire whip. The mixing speed was then increased to #10 for 3 min. Typically, after approximately 1 min at the high speed, the mixture would suddenly emulsify. The emulsion was then placed in a plastic mixing bowl and beat at high speed with a kitchen mixer for an additional 3 min, stopping every 45 seconds to scrape the sides of the bowl. Temperature at completion of mixing was typically 88 °C, well above the crystalization temperature of the salt solution (82 °C).

Numerous samples were taken for density measurements and examination under an optical microscope. Due to air entrainment during mixing, a good measure of the void-free emulsion density was not obtained. It was not possible to remove the entrained air by vacuum due to the stiffness of the emulsion. Techniques were developed later, after HMX/emulsion mixing, to remove most of the voids. A good measure of the void-free emulsion density was finally obtained by adding a known quantity of light mineral oil to reduce the stiffness of the emulsion which allowed the entrained air to escape. By measuring the density of the diluted emulsion and considering the density of the added mineral oil, the void-free density was determined to be 1.43 g/ml.

Figure 4 shows a typical microscope photograph of the emulsion at a power of 160X. Photographs were also taken at 160X of 10/90 HMX/emulsion mixtures to determine the effects of additional mixing of the emulsion matrix at room temperatures when loaded with a particulate. The emulsion cell size distribution was measured for each case and the

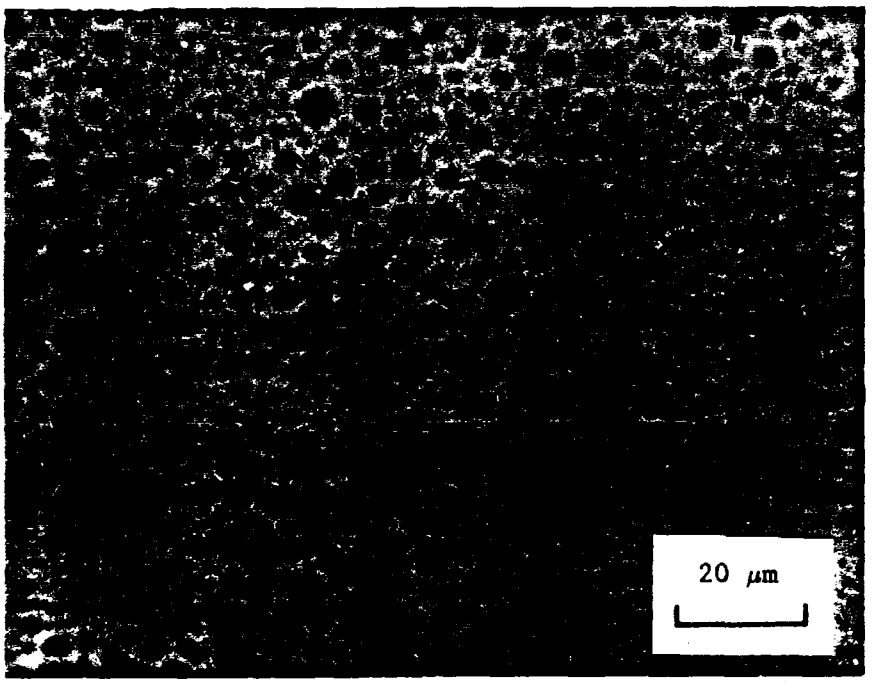

Figure 4. Microscope photograph of emulsion, 160X.

results in terms of frequency and mass were plotted in Figure 5. The frequency and mass are normalized but the results can be directly related to the actual frequency and mass distributions over the cell sizes. The results in Figure 5 are as expected. The nominal mass mean cell size of the pure emulsion is about 7 μm, and the effects of mixing in the HMX is to reduce the mass mean cell size of the emulsion to around 4 μm. It is assumed that higher loadings of HMX in the emulsion would result in even smaller cell sizes.

HMX/Emulsion Mixing Operations. The original plan for HMX/emulsion mixing was to produce mixtures ranging from 10% to 70% HMX using a blend of HMX grades composed of 35% fine and 65% coarse grade HMX. This particular blend was selected because (1) the grades necessary for this blend were available and (2) this was the blend selected by the Defense Nuclear Agency in the casting of 500-kg HMX charges using a propellant binder (85% HMX/15% binder). A 50/50 mix using only coarse grade HMX (50C/50) and another using only fine grade HMX (50F/50) were planned to investigate, in a very preliminary way, the effects of particulate size on detonation performance. As will be shown, this plan was revised immediately after mixing operations began.

The HMX blend was used initially in a 40/60 mix resulting in a very stiff matrix with the consistency of a soft, nontacky putty. Next, the 50F/50 mix was attempted, and the matrix apparently failed, resulting in a dry, lumpy noncohesive mix. A 1-kg batch of 50C/50 was prepared in a small blender resulting in a mix with the consistency of a stiff paste. It was then concluded that the fine grade HMX was presenting the emulsion (in particular, the continous phase of the emulsion) with excessive surface area. The decision was made to use only coarse grade HMX for the remaining mixes. The terminology was changed so that the coarse grade HMX had no identifying letter (such as "C") and the blend was identified by the letter B in the specification of the HMX/emulsion mixture ratio, i.e., 40B/60.

The remaining mixes were prepared using only coarse grade HMX. The 30/70, 20/80 and 10/90 mixes provided smooth matrices with decreasing

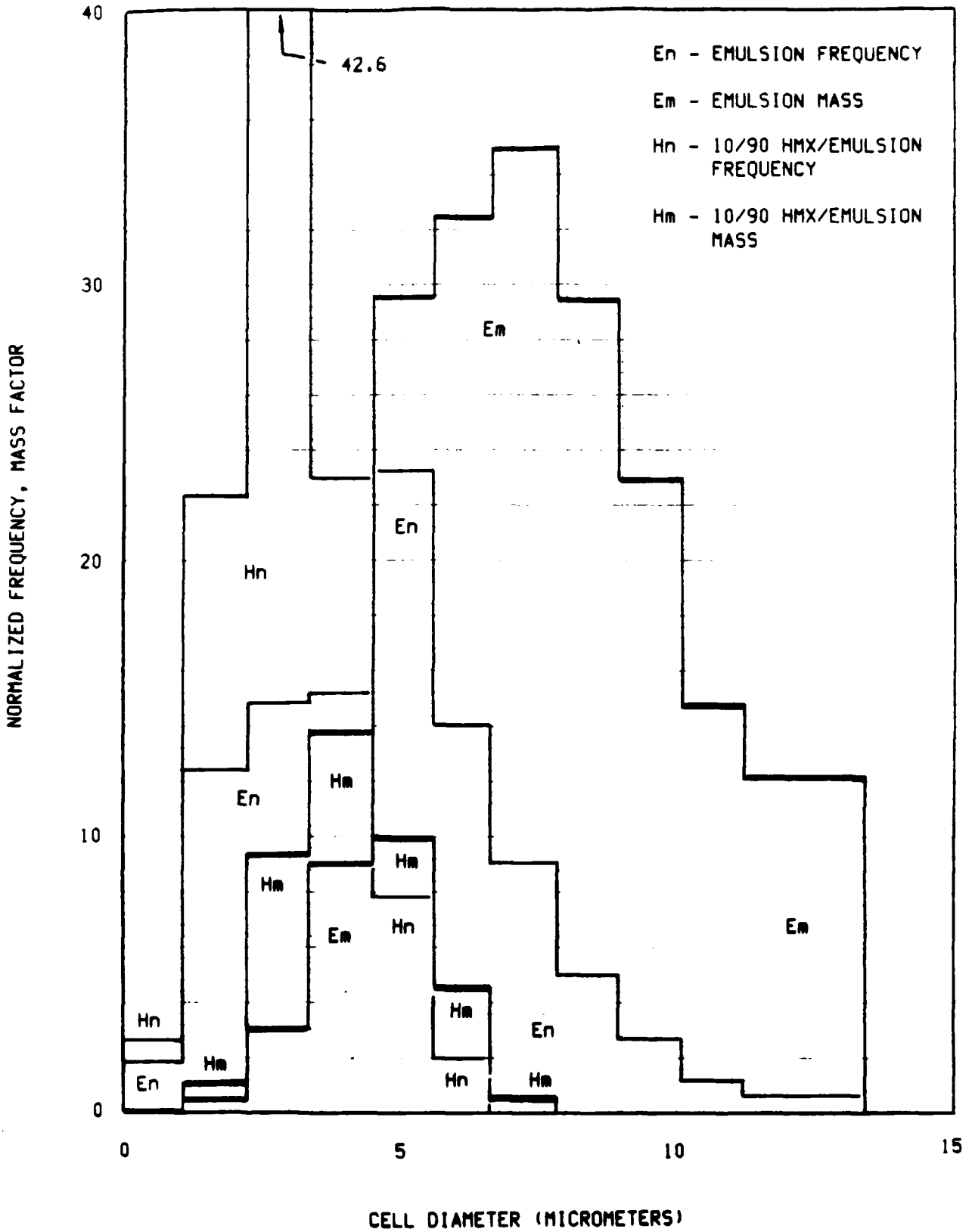

Figure 5. Emulsion cell size mass and frequency distribution for 100% emulsion and 10/90 HMX/emulsion mixture.

stiffness. The 70/30 mix had the consistency of a slightly damp noncohesive powder. A large quantity of 50/50 mix (several kg) was prepared resulting in the stiff paste as observed previously with the 1-kg 50/50 mix. However, within two days this mix solidified. It is suspected that, due to the high HMX loading, excessive shear during mixing resulted in matrix failure and crystalization of the salt solution. A 60/40 mix was not attempted due to a shortage of emulsion and the strong probability that a successful mix would not result.

A second mixing operation was conducted to (1) provide the 40/60 mix not obtained, during the initial mixing operation; (2) provide additional quantities of 20/80 and 50/50 mixes, and (3) attempt to obtain a good 60/40 mix. Care was taken this time to apply minimum shear, especially to the 50/50 and 60/40 mixes. A good 40/60 mixture was obtained; however, the 50/50 mix solidified as before and the 60/40 mix produced a dry but somewhat cohesive consistency, i.e., it could be packed to form a relatively stable mass. Thus, the experimental program proceeded with an insufficient quantity of 50/50 mix to conduct a 51.5-mm-diameter cylindrical charge experiment planned as part of the test matrix.

Coarse grade HMX size specifications are shown in Table 2. Table 3 presents the results of the hazards analysis testing performed by LANL for HMX/emulsion mixtures. A notable result of the data in Table 3 is the greatly reduced spark sensitivity for HMX/emulsion mixtures relative to pure HMX. HMX/emulsion mixtures of greater than 50% HMX show increased sensitivity to impact, though somewhat less so than pure HMX.

HMX/Emulsion Density Measurements. Density measurements were made by loading a small cup with the HMX/emulsion mixtures using the same techniques that were used in loading the charge containers. Details of the loading procedures will be discussed under **CHARGE LOADING.** The results are shown in Figure 6 where density is plotted as a function of percent HMX. The data plotted for the 40% HMX mixture are for the 40/60 mix. The density of the 40B/60 mix was essentially the same as that of the 40/60 mix. The density for the 60/40 mix lies slightly above the

Table 2. HMX specifications.

Class 2, Grade B, not greater than 2% RDX

SIEVE SIZE (um)	PERCENT PASSING
297	100
125	98
44	75

Table 3. Hazards analysis data.

	FORMULATION			
SENSITIVITY	75/25	50/50	25/75	0/100
Impact Sensitivity Type 13/138	35.6/100	43.5/95.5	320/>320	>320/>320
DTA				
Exotherm Peak (C)	236	236	240	240
Onset of Exotherm (C)	200	210	200	250
Pyrolysis (C)	256	258	264	270
Spark Sensitivity				
3 mil/10 mil (J)	1.73/4.1	---	---	1.90/8.4
Henkin Critical Temp (C)	209	---	---	300

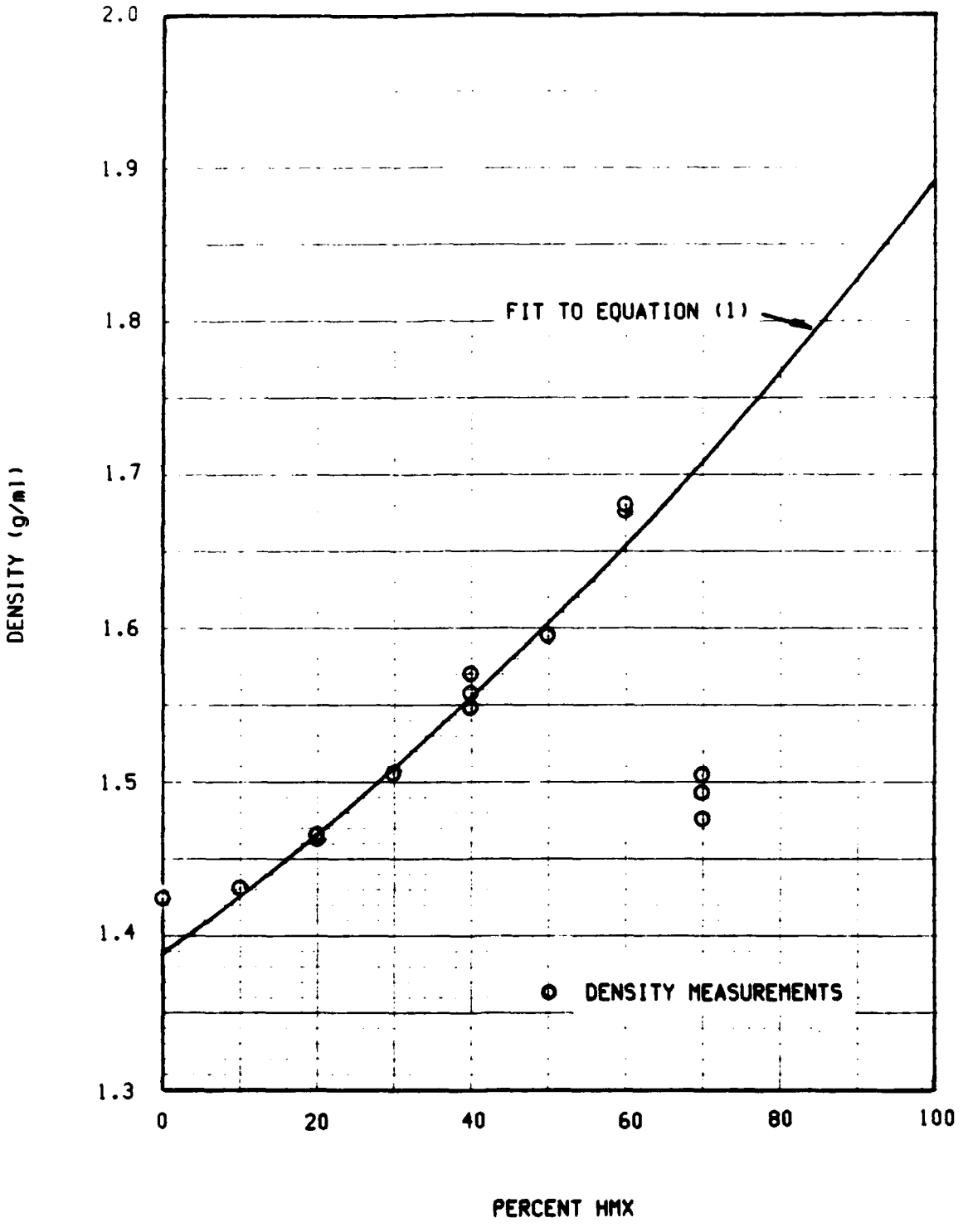

Figure 6. Variation of HMX/emulsion density with percentage HMX.

curve, probably because it had to be packed into the charge container which apparently drove some of the entrained air out. The density of the 70/30 mix lies well below the other data because the noncohesive nature of that mix made it impossible (at reasonable pressures) to pack the mix to form a mechanically stable mass.

The mixture equation which calculates the density, ρ_m, of a mixture of n components of densities $\rho_1, \rho_2, \ldots \rho_n$ and mass fractions $\chi_1, \chi_2, \ldots \chi_n$ is

$$\rho_m = \frac{1}{\chi_1/\rho_1 + \chi_2/\rho_2 + \ldots \chi_n/\rho_n} \qquad (1)$$

The curve shown in Figure 6 is a plot of equation (1) where the emulsion density, ρ_1, has been adjusted to provide the best fit to the data. The emulsion density which gave the best fit was $\rho_1 = 1.389$ g/ml. The standard density of 1.89 g/ml for HMX, ρ_2, was used. Recall that an emulsion density measurement was made where all of the entrained air was removed to obtain a density of 1.43 g/ml. This measurement, when compared to the value determined by the fit of Equation (1) to the data, implies that the HMX/emulsion mixing process consistently introduced air into the emulsion at a constant volume fraction of approximately 3%.

CHARGE LOADING

Various techniques were developed for loading of the test articles because of the range of matrix stiffnesses encountered for the various HMX/emulsion mixes. The smaller charge containers were loaded successfully with 10/90, 20/80, 30/70 and 40/60 mixtures using manually pressed frosting bags with a simple conical tip. For loading of the larger charges, a simple pressure vessel was constructed which forced the mixture into the containers under air pressure produced by a hand operated bicycle pump. These loading procedures worked quite well and, with only one notable exception, resulted in uniform void-free charges.

Due to the very stiff nature of the 40B/60, 50/50 and 60/40 mixtures, a completely different approach to test article loading was needed. A procedure which worked very well, even though somewhat tedious, was to drop small balls of the mixture approximately one-half the diameter of the bore and tamp it with a wooden dowel rod. For the conical charges, a similar procedure was used by loading from the large end using small balls and dowel rods initially and increasing their diameters as the conical container was filled.

Prior to filling a frosting bag or the pressure vessel, the mixture was smoothly spread over the surface of a one-quarter inch thick acrylic sheet using a rubber spatula. The mixture was worked to a thickness of approximately 1 to 2 mm. Visible clumps of HMX were removed (> 0.5 mm), and then the mixture was recovered from the acrylic sheet with a rubber spatula using a slow snowplow action. This procedure removed most of the larger air bubbles entrained in the mixture.

INSTRUMENTATION SYSTEMS

Electronic Measurements. The Big Eagle Facility is configured for electronic measurements of TOA from ionization and shorting pins, and voltage versus time measurements provided by resistance probes. A LeCroy Model 6900-1 Digital Oscilloscope and Instrumentation Control System[8] is the heart of the measurement system. An IBM PC with CATALYST software is used to set up recording channels and analyze data. For TOA measurements, a pulse-forming network provides the signal conditioning for recording on the LeCroy system. For resistance probe measurements, a constant current power supply is used to drive the resistance probe. Permanent digitized data records are provided on disks.

Streak Camera. Streak camera data were recorded on a Beckman & Whitley Model 770[9] rotating mirror camera. The camera records during 1/12 of the revolution of the mirror on a 200-mm length of 70-mm film. Rotor position and velocity are monitored by means of a pickup coil and

armature placed over a magnetized rotor shaft. The rotor is driven by a dry nitrogen turbine system.

Synchronization and control is accomplished by operator controls and synchronization electronics. A trigger pulse is produced which will initiate the event at some specified time increment in advance of the time at which the mirror image encounters the film leading edge. The system automatically produces the trigger pulse when the firing button is depressed and the turbine is up to speed.

SECTION 3
THEORETICAL CALCULATIONS

Theoretical calculations were performed for HMX/emulsion mixtures over the range of from 100% emulsion to 100% HMX. Calculations were performed using the TIGER code with the BKWR equation of state which utilizes the revised BKW parameters developed by Mader[10] in fitting calculational results to experimental data for RDX. Since the thermodynamic modeling in TIGER gives no consideration to geometry and size, the results are essentially representative of those for an infinite diameter charge for planar detonation. Thus, comparisons of theoretical and experimentally determined detonation velocities must be made based on extrapolations of experimental results to infinite diameter.

Mixture densities used in the calculations are based on the experimental results shown in Figure 6. The TIGER library did not contain constituent data (molecular composition, enthalpy of formation, molar volume, state reference, specific heat) for light mineral oil and the emulsifier, PSA, so substitutions were made from the existing library. Paraffin is an excellent representation of light mineral oil and data for a standard commercially available emulsifier, Span 80, was used as an approximation for PSA.

The constituents for the calculations are summarized in Table 4. The results of the calculations are summarized in Table 5.

The oxygen balance calculations in Table 5 were performed separately from the TIGER calculations and assume that all available oxygen reacts to form CO_2 and H_2O. A small code written in BASIC called BALANCE was developed to perform the calculations. A listing of BALANCE is provided in the appendix.

The calculational and experimental results will be compared in Section 4.

Table 4. HMX/emulsion constituents for TIGER calculations.

MIX (HMX/EMUL)	DENSITY (g/ml)	HMX	AN	SN	H2O	PARAFFIN	SPAN 80
0/100	1.389	0	.7150	.1000	.1200	.0183	.0467
10/90	1.427	.10	.6435	.0900	.1080	.0165	.0420
20/80	1.467	.20	.5720	.0800	.0960	.0146	.0374
30/70	1.509	.30	.5005	.0700	.0840	.0128	.0327
40/60	1.554	.40	.4290	.0600	.0720	.0110	.0280
50/50	1.601	.50	.3575	.0500	.0600	.0092	.0233
60/40	1.652	.60	.2860	.0400	.0480	.0073	.0187
70/30	1.705	.70	.2145	.0300	.0360	.0055	.0140
80/20	1.763	.80	.1430	.0200	.0240	.0037	.0093
90/10	1.824	.90	.0715	.0100	.0120	.0018	.0047
100/0	1.890	1.00	0	0	0	0	0

Table 5. Results of HMX/emulsion TIGER calculations.

MIX (HMX/EMUL)	DENSITY (g/ml)	CJ PRESS (GPa)	DET VEL (km/s)	TEMP (K)	OXY BAL (%)
0/100	1.389	15.47	6.930	1777	2.45
10/90	1.427	18.02	7.321	2041	.04
20/80	1.467	19.82	7.529	2154	-2.36
30/70	1.509	21.69	7.726	2261	-4.77
40/60	1.554	23.70	7.916	2363	-7.18
50/50	1.601	25.91	8.098	2467	-9.59
60/40	1.652	28.18	8.292	2574	-11.99
70/30	1.705	30.60	8.484	2680	-14.40
80/20	1.763	33.29	8.687	2782	-16.81
90/10	1.824	36.14	8.894	2883	-19.21
100/0	1.890	39.28	9.116	2980	-21.62

SECTION 4
RESULTS AND DISCUSSION

SUMMARY OF EXPERIMENTAL RESULTS

The experimental results are summarized in Tables 6 through 9. In Table 6 the results are shown in terms of whether or not successful detonation was achieved for each cylindrical charge experiment. Table 7 presents the same results for the conical charge experiments.

Table 8 summarizes the experiments conducted at the Big Eagle Facility and Table 9 summarizes those conducted at the Little Eagle Facility. Experiments designed for electronic TOA and resistance probe measurements were conducted at Big Eagle. Experiments designed for streak camera photography were conducted at Little Eagle.

Most of the experiments were straightforward and the results are adequately described in the tables. For a few experiments, additional remarks are required as follow:

BE87-118. This was a conical charge experiment for the 20/80 mix in which resistance probe measurements were made to determine detonation velocity and failure diameter. Good resistance data were obtained; however, improper voltage offset on the recording instrumentation permitted recovery of only the later portions of the data.

BE87-121. This experiment was a repeat of BE87-118. Voltage offset was corrected and good resistance data were obtained. In loading the test article, however, there was a shortage of the 20/80 mix and 150 mm of 30/70 mix was required to complete filling of the driver section. Erratic behavior of the detonation velocity in the conical section was probably caused by the long section of 30/70 mix in the driver.

Table 6. Cylindrical charge test matrix.

HMX/Emul

DIAMETER (mm)	70/30	60/40	50/50	40B/60	40/60 (a)	30/70	20/80	10/90 (b)
51.50	---	---	---	---	O	O	O	---
26.10	---	---	O	O O	O	O O	X X	X
12.55	---	O	O	O O	O O	X X	---	---
6.35	O O	X	X	---	---	---	---	---
3.18	---	X	---	---	---	---	---	---

O GOOD SHOT X DETONATION FAILURE --- NO TEST

(a) Plate dent test at 41.28-mm diameter not included
(b) Plate dent test at 101.6-mm diameter not included

Table 7. Conical charge test matrix.

HMX/Emul

CONICAL SECTIONS	70/30	60/40	50/50	40B/60	40/60	30/70	20/80	10/90
I - II	---	---	---	---	---	---	0 0 0	X
II - III	---	---	---	0	---	0 0 (a)	---	---
III - IV	---	---	0 0	0	0	---	---	---

0 GOOD SHOT X DETONATION FAILURE --- NO TEST

SECTION I: 50.80 - 25.40 mm
SECTION II: 25.40 - 12.70 mm
SECTION III: 12.70 - 6.35 mm
SECTION IV: 6.35 - 3.18 mm

(a) Section II only on second test

Table 8. Big Eagle experiments.

SHOT NO.	CONFIGURATION	COMPOSITION % HMX/EMUL	DIAMETER (mm)	DENSITY (gm/ml)	RESULTS
BE87-110	CYLINDRICAL	10/90	26.10	1.426	DETONATION FAILURE
BE87-111	CYLINDRICAL	20/80	26.10	1.466	DETONATION FAILURE
BE87-112	CYLINDRICAL	30/70	26.10	1.510	D = 6.298 (+.045/-.040) mm/us (a)
BE87-113	CYLINDRICAL	20F/80	26.10	1.466	DETONATION FAILURE
BE87-114	CYLINDRICAL	40B/60	26.10	1.554	NO PIN DATA
BE87-115	CONICAL	10/90	50.8-12.7	1.426	DETONATION FAILURE
BE87-116	CYLINDRICAL	50/50	26.10	1.602	D = 7.768 (+.132/-.161) mm/us
BE87-116	CYLINDRICAL	40B/60	26.10	1.554	D = 7.132 (+.194/-.205) mm/us
BE87-116	CYLINDRICAL	30/70	26.10	1.510	D = 6.132 (+.137/-.112) mm/us

(continued)

Table 8. Big Eagle experiments.
(continued)

SHOT NO.	CONFIGURATION	COMPOSITION % HMX/EMUL	DIAMETER (mm)	DENSITY (gm/ml)	RESULTS
BE87-117	CYLINDRICAL	50/50	12.55	1.602	D = 7.430 (+.146/-.184) mm/us
BE87-117	CYLINDRICAL	40B/60	12.55	1.554	D = 6.548 (+.041/-.033) mm/us
BE87-117	CYLINDRICAL	30/70	12.55	1.510	DETONATION FAILURE
BE87-118	CONICAL	20/80	50.8-12.7	1.466	df = 14.7 - 17.5 mm
BE87-119	CYLINDRICAL	30/70	51.50	1.510	D = 6.959 (+.044/-.062) mm/us
BE87-120	CYLINDRICAL	20/80	51.50	1.466	D = 5.514 (+.027/-.029) mm/us
BE87-121	CONICAL	20/80	50.8-12.7	1.466	(b) df = 30 mm
BE87-122	CYLINDRICAL	40B/60	12.55	1.554	D = 6.740 (+.125/-.101) mm/us
BE87-122	CYLINDRICAL	30/70	12.55	1.510	DETONATION FAILURE

(continued)

Table 8. Big Eagle experiments.
(concluded)

SHOT NO.	CONFIGURATION	COMPOSITION % HMX/EMUL	DIAMETER (mm)	DENSITY (gm/ml)	RESULTS
BE87-236	CYLINDRICAL	40/60	26.10	1.554	D = 6.871 (+.016/-.033) mm/us
BE87-237	CYLINDRICAL	40/60	12.55	1.554	D = 6.360 (+.078/-.081) mm/us
BE87-237	CYLINDRICAL	40/60	12.55	1.554	D = 6.155 (+.154/-.132) mm/us
BE87-238	CYLINDRICAL	60/40	12.55	1.652	D = 7.802 (+.047/-.098) mm/us
BE87-239	CYLINDRICAL	40/60	51.50	1.554	D = 7.375 (+.072/-.044) mm/us
BE87-240	CONICAL	20/80	50.8-12.7	1.466	df = 18.5 - 19.4 mm (c)
BE87-241	CYLINDRICAL	40/60	41.28	1.554	PLATE DENT, P = 234 kbar
BE87-242	CYLINDRICAL	10/90	101.60	1.426	PLATE DENT, P = 74 kbar

(a) ± indicates variation in velocities calculated from multiple TOA measurements. Uncertainties for all calculated velocities are less than ± 0.5%.
(b) Unreliable measurement, see text for discussion.
(c) Based on posttest inspection of resistance probe.

Table 9. Little Eagle experiments.

SHOT NO.	CONFIGURATION	COMPOSITION % HMX/EMUL	DIAMETER (mm)	DENSITY (gm/ml)	RESULTS
LE87-126	CONICAL	50/50	12.7-3.18	1.602	df = 5.7 - 8.1 mm
LE87-127	CONICAL	40B/60	25.4-6.35	1.554	df = 7.1 - 8.6 mm
LE87-128	CONICAL	40B/60	12.7-3.18	1.554	df = 8.4 - 9.8 mm
LE87-129	CONICAL	30/70	25.4-6.35	1.510	df = 9.8 - 11.9 mm
LE87-130	CYLINDRICAL	50/50	6.35	1.602	DETONATION FAILURE
LE87-131	CONICAL	50/50	12.7-3.18	1.602	df = 5.8 - 6.6 mm

(continued)

Table 9. Little Eagle experiments.
(concluded)

SHOT NO.	CONFIGURATION	COMPOSITION % HMX/EMUL	DIAMETER (mm)	DENSITY (gm/ml)	RESULTS
LE87-136	CYLINDRICAL	70/30	6.35	1.500 (a)	D = 6.95 mm/us
LE87-136	CYLINDRICAL	70/30	6.35	1.500 (a)	D = 6.86 mm/us
LE87-137	CONICAL	40/60	12.7-3.18	1.554	df = 7.6 - 9.1 mm
LE87-138	CONICAL	30/70	25.4-12.7	1.510	FAILURE NOT OBSERVED
LE87-139	CYLINDRICAL	60/40	6.35	1.652	DETONATION FAILURE
LE87-140	CYLINDRICAL	60/40	3.18	1.652	DETONATION FAILURE

(a) approximate

BE87-240. This experiment was a repeat of BE87-118 and -121. In this experiment, erratic resistance probe data were observed. This was probably caused by air bubbles that were inadvertently introduced when problems were encountered during charge loading operations. A good estimate of failure diameter was made, however, by measuring the position of the mechanical short in the resistance probe which was recovered posttest.

BE87-114. No pin data were recovered. No explanation could be found for this loss of data.

In most cases, charges were initiated with an RP-80 and 8 mm of Deta-Sheet. For mixes of 30/70 and less (less HMX), an additional layer of several millimeters of 40B/60 was added for additional boosting.

Good ionization pin signals were observed for mixtures of 40/60 and greater. Adequate signals were observed for 30/70 mixes, but erratic signals were observed in the initial 20/80 experiments. In later 20/80 experiments, shorting pins which rely on mechanical shorting from pressure effects, rather than on ionization effects, were used to register arrival time of the detonation front.

DATA ANALYSIS METHODS

A brief review of the analysis methods used to reduce the data will be presented. This review will include the analysis for TOA, resistance probe, streak camera and plate dent data.

TOA Analysis. By making four TOA measurements, six velocities can be calculated. The detonation velocity results in Table 8 indicate the average of the six velocities with the maximum and minimum variations about the average indicated by the ± values. In some cases only three TOAs were recorded, resulting in only three calculated velocities. As indicated previously, the uncertainty in any given calculated value of

detonation velocity based on TOA measurements is less than 0.5%. Representative ionization pin data are shown in Figure 7.

Resistance Probe Analysis. Voltage-time data were recorded on the Lecroy system. The change in position of the shock-induced mechanical short in the resistance probe, Δx, is directly related to the change in voltage, ΔV, through the relation

$$\Delta x = \Delta V/(kI) \qquad (2)$$

where k is the wire resistance per-unit-length (0.2809 Ω/mm) and I is the current. The voltage-time data may be differentiated at various positions to determine the variation of detonation velocity with x. Detonation failure is indicated by an abrupt change in slope of the voltage-time data or by first indication of constant voltage. Figure 8 shows the results of a resistance probe experiment, BE87-118. The data were analyzed and processed using the Lecroy CATALYST program on an IBM PC.

Independent TOA measurements are made at several positions to establish a precise position-time reference for the resistance probe data. Since the position of the pins and the times at which the detonation front arrives at the pins are precisely known, a direct relation can be established between the recorded voltage and pin positions. Without this information, $\Delta V/\Delta t$ could still be accurately determined but the position along the charge axis at which that value of $\Delta V/\Delta t$ occurred could not be precisely determined.

From the geometry of the conical charges the diameter at any position along the axis is precisely known and is calculated from the relation

$$d = d_1 - 0.05237\ x \qquad (3)$$

where d_1 is the charge diameter at the entrance to the conical section and x is the distance from the beginning of the conical section to the

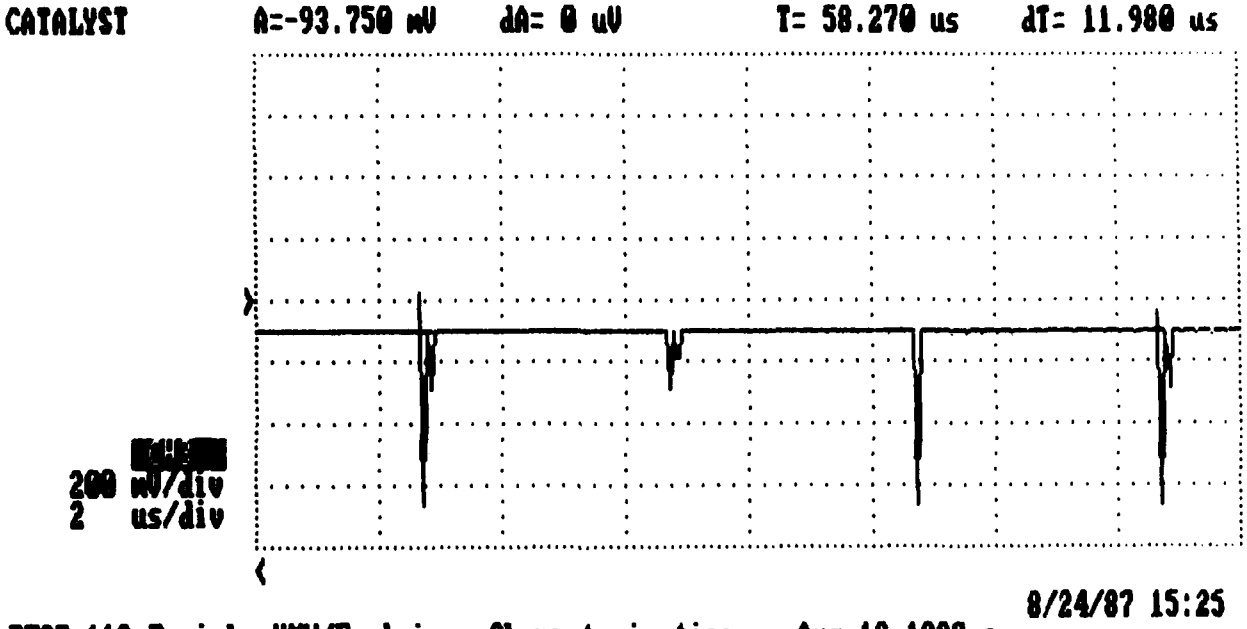

Figure 7. Ionization pin data, BE87-112.

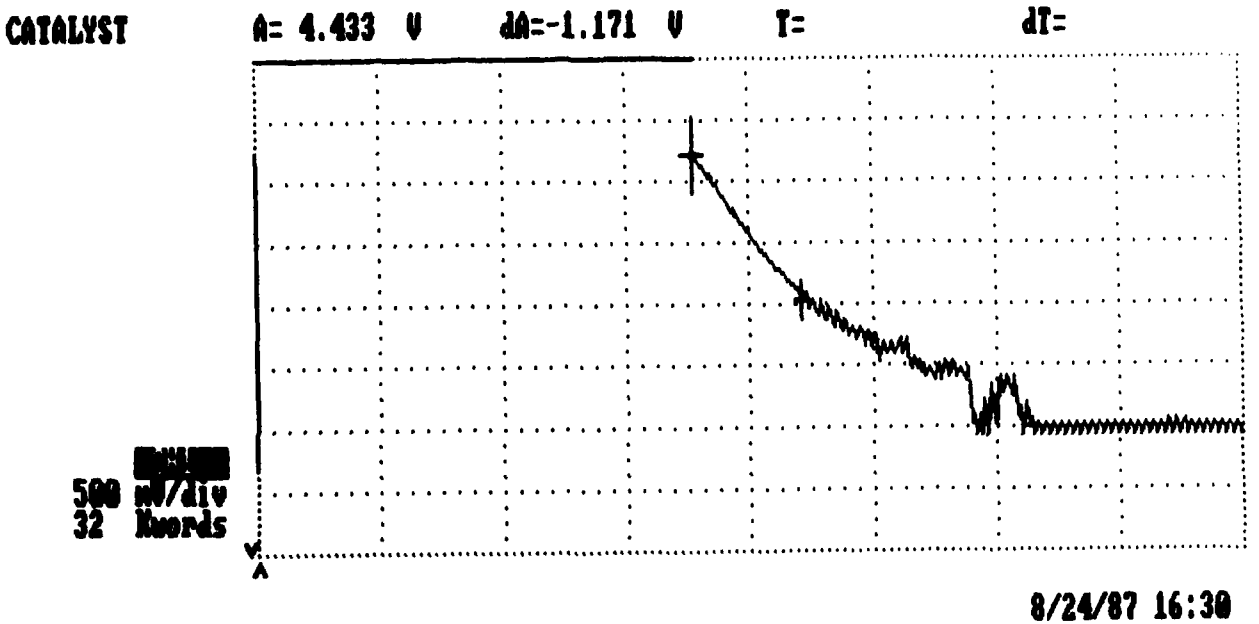

Figure 8. Resistance probe data, BE87-118.

location where the diameter is d. The coefficient is based on a conical angle of 3 degrees.

Craig[11] has shown that an overshoot in the propagation of detonation along the charge axis of up to one charge diameter can occur at detonation failure. This occurs because the detonation at any given station along the axis of a conical charge is always slightly overdriven. Thus, conical charge data tends to indicate failure at a diameter that is slightly smaller than the true failure diameter. The lower bound on failure diameter determined in the conical charge experiments has been adjusted to reflect this overshoot.

Streak Camera Photography. The length calibration along the axis of the charges in the streak camera experiments was established by making a still photo of the test article and using the known length of the test article (or a millimeter scale included in the photo) as the reference. The time base was established through the precisely known geometry of the film plane radius relative to the rotor axis and the rotor speed. Thus, the film writing speed, W, is determined as

$$W = 4\pi rn \qquad (4)$$

where r is the film plane radius and n is the rotor speed in rev/sec. Writing speed as determined above is accurate to within 0.25%. The film was read using a modified fiche reader. The effects of detonation overshoot at failure are considered in determining the failure diameter and equation (3) applies as before.

Plate Dent Analysis. A simple empirical technique has been developed by Smith[12] to obtain a rough determination of CJ pressure in an explosive. The experimental setup consists of a cylindrical charge positioned in the center of, and normal to, a steel plate which has been calibrated against known explosives. The CJ pressure for the explosive is determined by measuring the depth of the dent produced by detonation of the charge. The relationship between dent depth and CJ pressure is

$$P_{CJ} = F\ y \qquad (5)$$

where F is a factor which is related to the charge diameter, y is the dent depth in millimeters and P_{CJ} is in kbar. The values of F used in the two plate dent experiments (BE87-241 and -242) are F = 34.81 for a diameter of 41.28 mm and F = 8.67 for a diameter of 101.6 mm.

BE87-241 was conducted on the 40/60 mix at a diameter of 41.28 mm. A dent depth of 6.73 mm was measured which results in a calculated CJ pressure of 234 kbar (23.4 GPa). This is in good agreement with the CJ pressure calculated with TIGER of 237 kbar (23.7 GPa). The good agreement between experiment and calculation may be due to the fact that, at this diameter, the 40/60 mix is approaching ideal behavior and the heavy HMX loading makes the BKWR parameters appropriate for "RDX-like" explosives.

BE87-242 was conducted primarily as a go, no-go experiment for the 10/90 mix at a diameter of 101.6 mm. A witness plate was used to confirm detonation and provide an estimate of CJ pressure. Dent depth was measured in this experiment at 8.59 mm which results in a calculated CJ pressure of 74 kbar (7.4 GPa). This is well below the theoretical CJ pressure of 180 kbar (18.0 GPa) calculated with TIGER. This suggests that significant diameter effects affected the results of this experiment even at the large diameter. In addition, the 10/90 mix may be more "composite-like" than "RDX-like", in which case the BKWR parameters are less appropriate than for the 40/60 case above.

DISCUSSION

Detonation Velocity-Diameter-Mixture Analysis. The results in Tables 8 and 9 are plotted in Figures 9 through 12. In Figure 9 detonation velocity as a function of inverse charge diameter is plotted for the five HMX/emulsion mixtures for which data were obtained. In Figure 10 the logarithms of the absolute values of the slopes of the linear portions of the lines of constant mixture in Figure 9 are plotted as a function of percentage HMX as a means for better understanding the

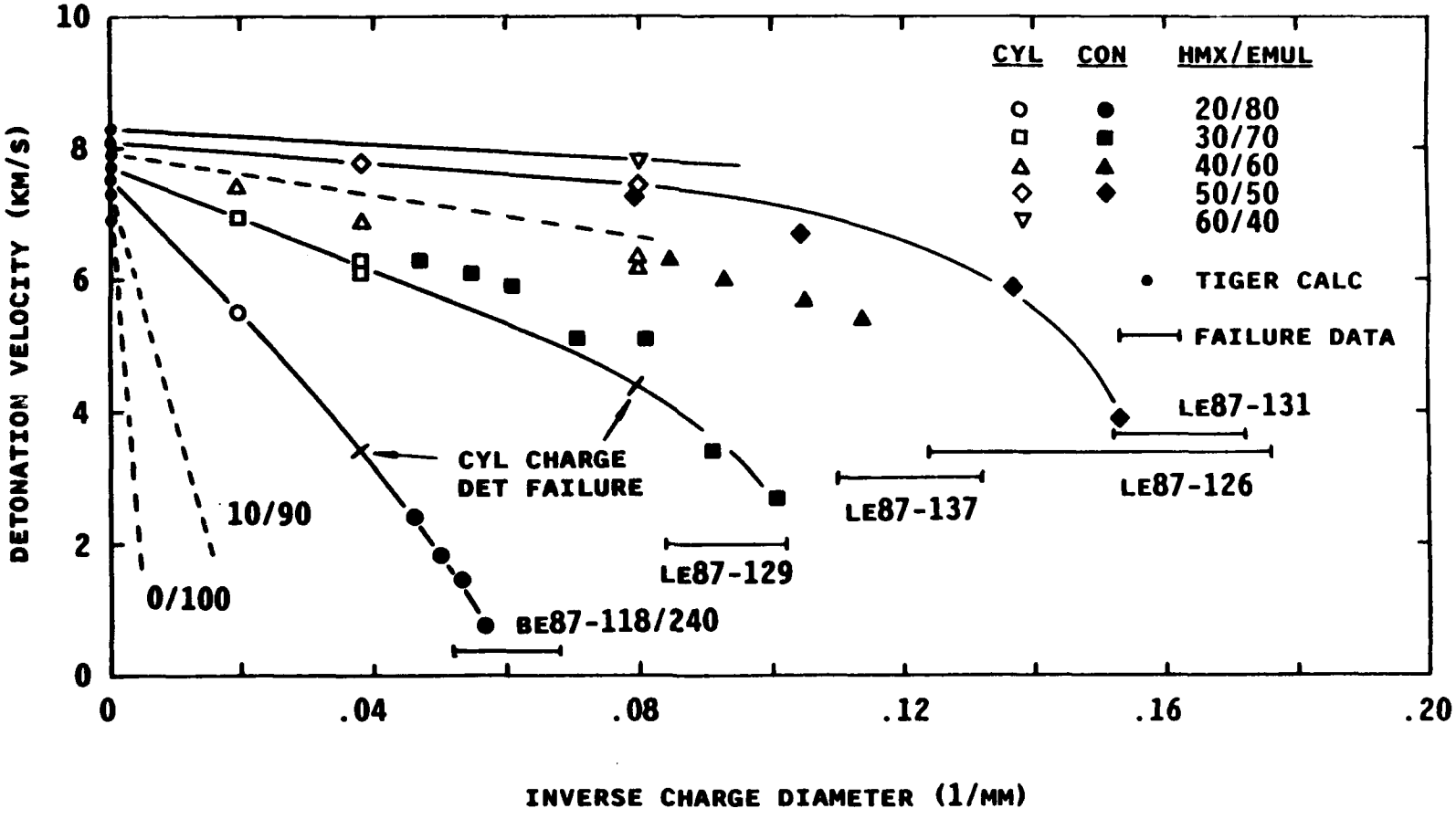

Figure 9. Detonation velocity versus inverse charge diameter for various percentages of HMX.

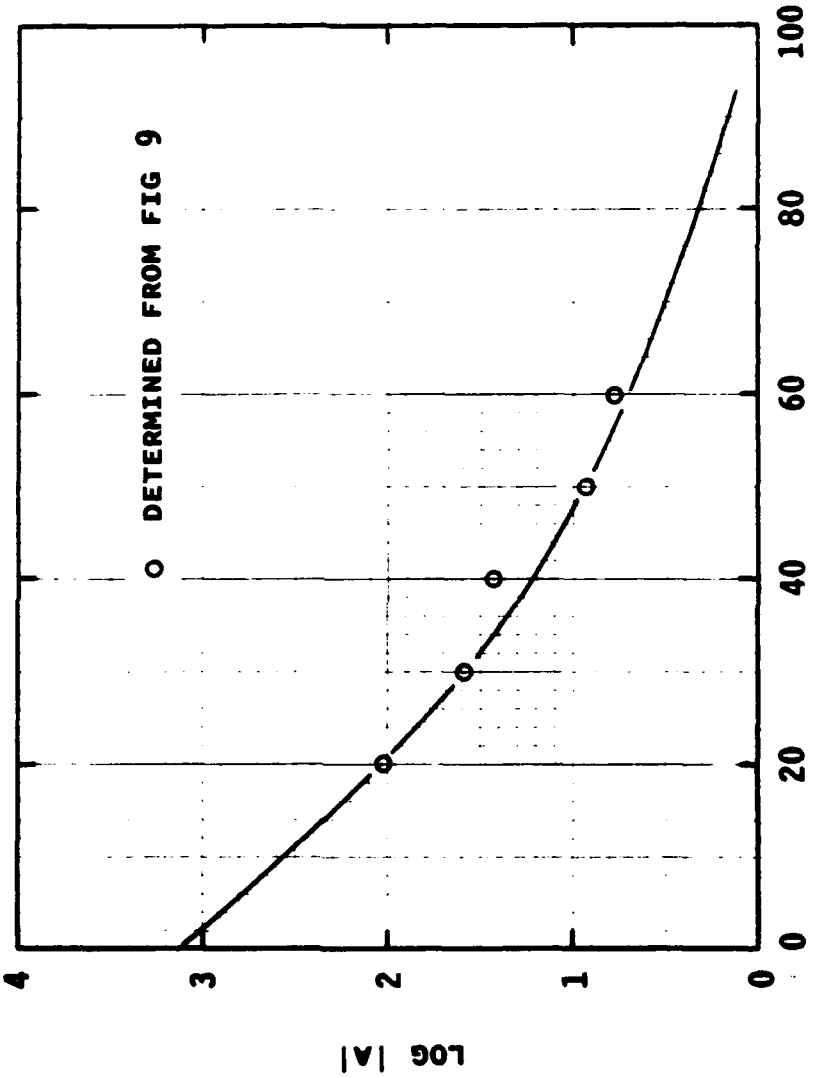

Figure 10. Plot of logarithm of absolute value of A (slope of D vs 1/d at large diameters from Figure 9) vs percentage HMX.

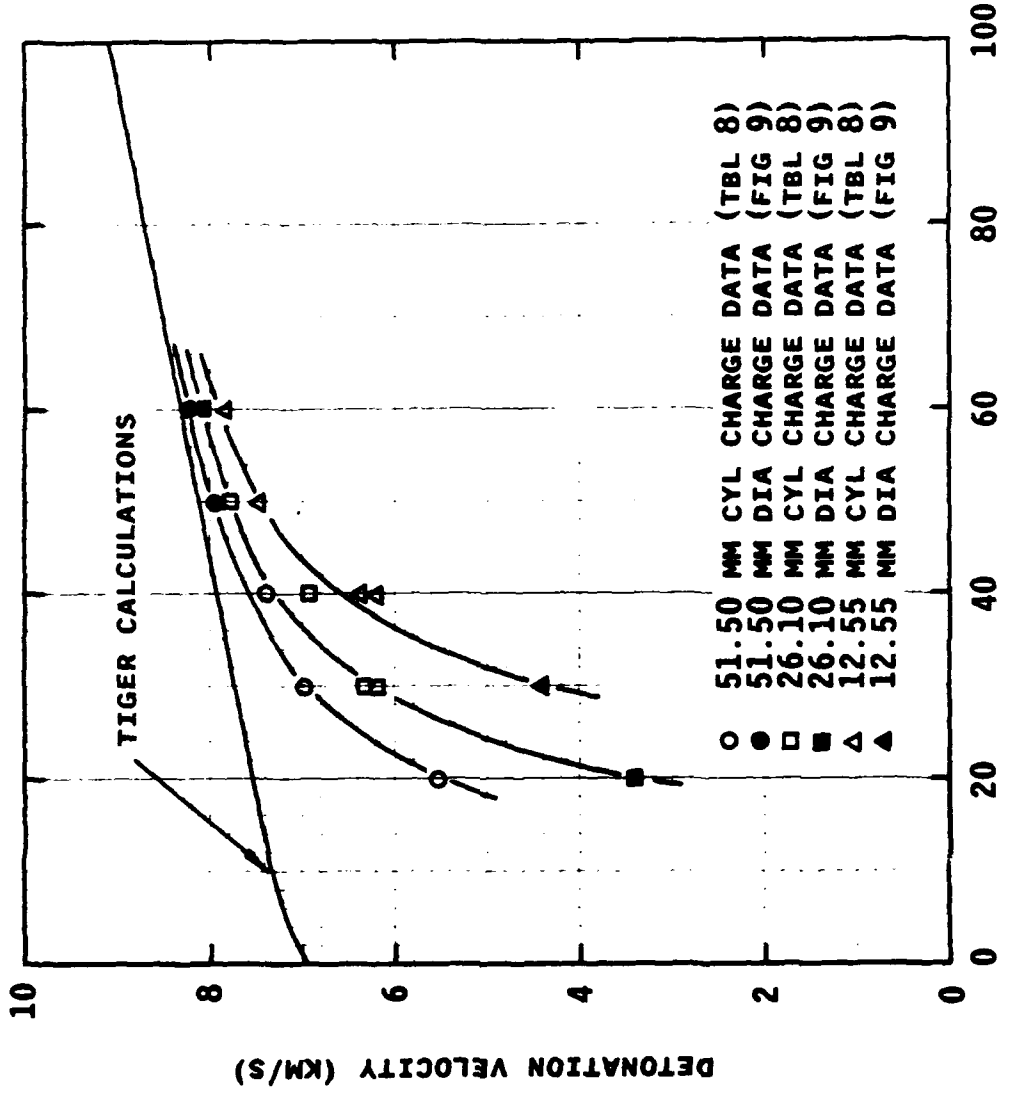

Figure 11. Detonation velocity as a function of percentage HMX for diameters of 12.55 mm, 26.10 mm and 51.50 mm.

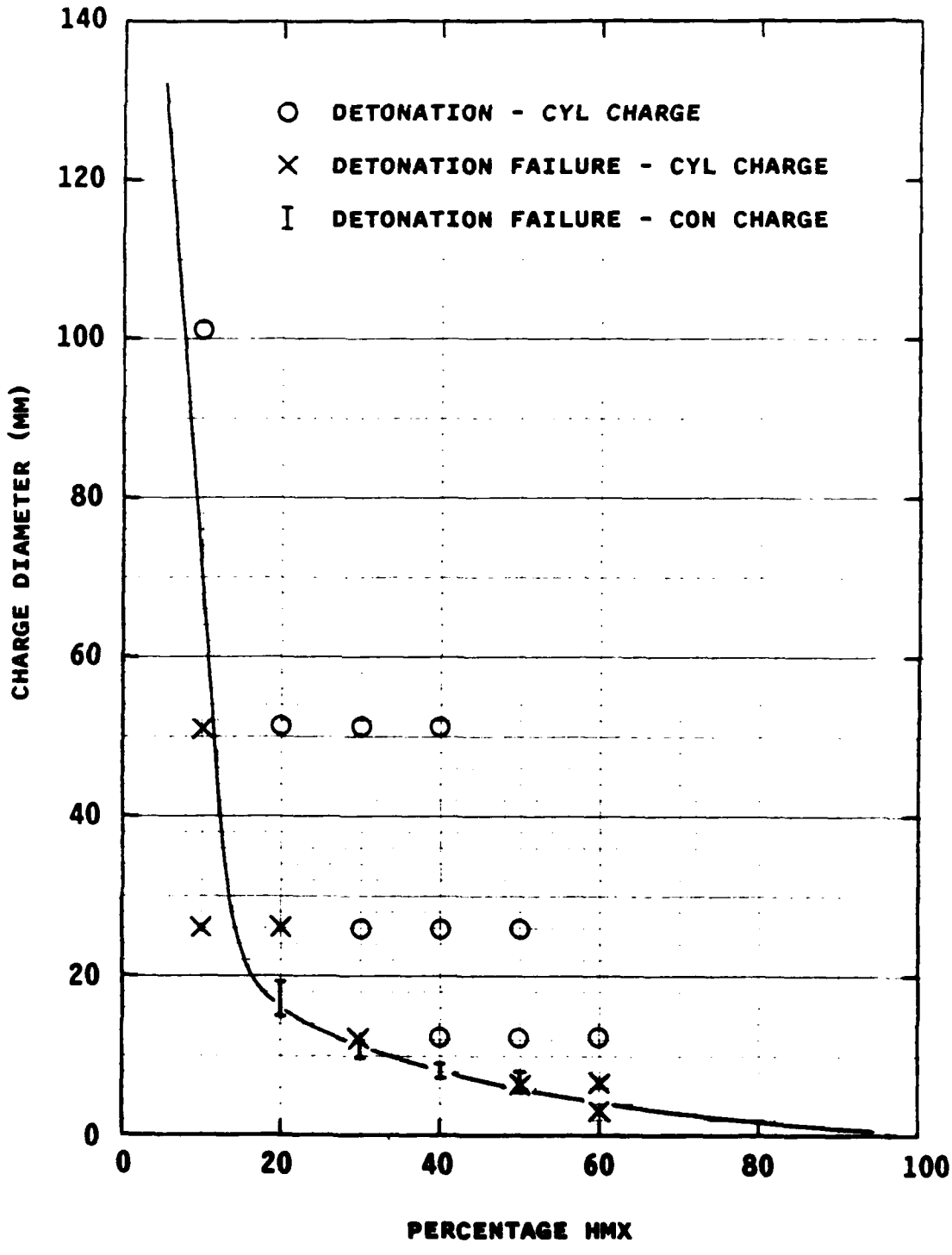

Figure 12. Definition of detonation failure envelope.

trends in the data. In Figure 11 detonation velocity as a function of percentage HMX is plotted for the three diameters for which data were obtained. In Figure 12 the boundary between regions of detonation and detonation failure is estimated by plotting the results of the cylindrical and conical charge experiments in charge diameter-percentage HMX space.

Figure 9 provides a comprehensive description of the results of the cylindrical and conical charge experiments. Detonation velocity is plotted as a function of inverse charge diameter for each HMX/emulsion mixture. The open symbols are data from Table 8 for the cylindrical charges. The solid symbols are points read from streak camera film records and resistance probe data for the conical charges. The horizontal bars are estimates of failure diameter based on interpretation of the streak camera film records and resistance probe data. In the streak camera film records, indications of possible detonation failure are a sudden change in slope of the record or a sudden change of light intensity. In the resistance probe data, indications of possible detonation failure are a sudden change in the slope of the voltage-time record or the sudden occurrence of constant voltage. While the results in some cases contain large uncertainties in failure diameter, the results in Figure 12 appear somewhat exaggerated because they are plotted as inverse charge diameter.

Figure 9 shows that, for a given mixture, a straight line through the cylindrical charge data, extrapolated to the infinite diameter (TIGER) velocity represents the results very well. This is consistent with the behavior of numerous molecular explosives as shown by Campbell and Engelke[13]. It is reasonable to assume that for diameters significantly larger than failure diameter, there is a consistancy, or as stated by Campbell and Engelke, a "regularity," in the relationship between slopes of constant mixture and percentage HMX. These slopes in Figure 9 were measured and the logarithm of their absolute values plotted against percentage HMX in Figure 10. Because the detonation velocities of the 40/60 mixture appeared to be anomalously low relative to the other mixtures, a straight line fit to that data in Figure 9 was

not made. However, the slope of a line through that data was measured and those results included in Figure 10, the purpose being to confirm the suspected "irregularity" of that data.

Some discretion has been exercised in deciding how best to fit the data in Figure 10. Giving preference to the 20, 30 and 50 percent HMX data, a curve has been fit by hand, recognizing that the slope of the 100 percent HMX mixture is very nearly zero and thus influences the behavior of the curve for mixtures greater than 60 percent in the manner shown. For mixtures of less than 20 percent HMX the curve has simply been extrapolated to the pure emulsion where the only constraint on the result is that the slope must be finite. Results in this region can only be treated as an estimate.

The results in Figure 10 clearly show that the 40/60 mixture data are deviant. However, the results can also be used to provide an estimate of what the slope of the 40/60 mixture should be for consistency. This estimate is indicated in Figure 9 with a dashed line. In addition, the results of Figure 10 have also been used to provide an estimate of the slopes for 10 percent HMX and the pure emulsion. These results are also shown in Figure 9 as dashed lines.

In principle it is possible to use the results shown in Figure 9 (horizontal bars) to determine the detonation velocity at failure for each mixture. However, due to the large negative slopes at and near failure, and, in some cases, the large uncertainties in estimates of failure diameter, it is not possible to provide a definition of the failure boundary with any degree of confidence. A general observation can be made, however, that for low percentage HMX mixtures failure occurs at large diameters at low velocities, while for high percentages HMX mixtures failure occurs at small diameters at high velocities. This result is in qualitative agreement with the behavior indicated in Figure 1.

The short lines crossing the 20/80 and 30/70 data in Figure 9 indicate that at those diameters detonation was not observed in

cylindrical charge experiments. Since the results of the 20/80 and 30/70 conical charge experiments indicate detonation at smaller diameters, the adequacy of the boosters used to initiate these charges becomes suspect.

Figure 11 shows variation of detonation velocity with percentage HMX for constant diameter. The results of the TIGER calculations (Table 5) are included. As shown, charges with higher percentage HMX and larger diameters result in increased detonation velocity as well as a closer approach to the TIGER results which are assumed to be a good estimate of detonation velocity as infinite diameter. The open symbols are plots of the results from Table 8 for the cylindrical charges. The solid symbols are plots of points determined from Figure 9 which could be determined with good confidence. Because of the limited data and large uncertainties in velocity at failure, no attempt has been made in Figure 11 to establish the detonation failure boundary. As noted before, qualitative agreement with the behavior described in Figure 1 is demonstrated.

In Figure 12 an estimate of the detonation failure envelope was made by constructing a curve between the regions of detonation and detonation failure. The curve shown was constructed assuming that 100 percent HMX fails at less than 1-mm diameter and that this limit dominates the behavior of the curve for high-percentage HMX mixtures. The curve is only approximately defined and additional experiments would be required to precisely define the boundary, especially for mixtures where the HMX content is less than 40 percent. The 40/60 data have been included here even though prior analysis indicated that the measured detonation velocities are anomalously low relative to the other mixtures. Preference has been given to the conical charge data over the cylindrical charge data in constructing the curve. Note that two cylindrical charge data points indicating failure lie well within the detonation region. These are the same two points indentified in Figure 9 which may have been inadequately boosted. Questions about adequacy of initiation may apply to other cylindrical charge data as well. It is felt that the curve in Figure 12 is reliable to within ± 15 percent for

mixtures containing more than 20 percent HMX. For mixtures containing less than 20 percent HMX the curve can be treated only as an estimate. A precise determination of the failure for pure emulsion would remove much of the uncertainty in this region.

Diameter Effect Analysis. The diameter effect analysis of Campbell and Engelke[13] was applied to the 50/50 mixture data in Figure 9. Campbell and Engelke determined that the following functional form was descriptive of the behavior of a large number of heterogeneous explosives in a cylindrical geomety,

$$D=D_i[1-A/(R-R_c)] \qquad (6)$$

where D_i is the detonation velocity at infinite diameter, R is the charge radius and A and R_c are length parameters. The 50/50 mixture was selected for this analysis because the data were sufficient to provide a reasonable definition of the downward concavity of the D vs 1/d relationship near detonation failure. Four points on the D vs 1/d curve from Figure 9 were selected and fit by equation (6). The results are shown in Table 10 where the values of D/D_i calculated from the fit are compared with the experimentally determined values. As shown, a reasonable fit is achieved.

If equation (6) is descriptive of all other HMX/emulsion mixtures (there is no reason to think that it isn't) and the Campbell and Engelke regularities are present in the data (they should be), then a generalized description or model of the diameter effect for HMX/emulsion mixtures should be achievable by defining the dependence of A and R_c on percentage HMX. This generalized model will not be pursued here but should be addressed in future analysis.

HMX Particle Size Effects. Some remarks are in order concerning the 40/60 and 40B/60 mixtures. In the revised test matrix all mixtures utilized only the coarse grade HMX. The role of the 40B/60 mixture in the revised test matrix was to demonstrate (in a very preliminary way) the effect of fine grade HMX on detonation performance. The rationale

Table 10. Results of diameter effect analysis.
$A = 0.25$, $R_c = 2.8$, $D_i = 8.098$ km/s

DATA			EQUATION (6)	PERCENT ERROR
R(mm)	D(km/s)	D/D_i	D/D_i	
3.27	3.877	.479	.468	-2.2
4.17	6.607	.816	.817	-
6.28	7.430	.918	.928	1.1
13.05	7.768	.959	.976	1.8

in addressing this objective became somewhat confused when the detonation velocities of the 40/60 mixture were determined to be anomalously low. Undoubtedly, failure diameter and the D vs 1/d behavior (Figure 9) are affected and the meaningfulness of a comparison with the 40B/60 data becomes questionable. As indicated in Table 9, there is no clear difference in diameter at failure between the two (LE87-127/128 and LE87-137), though the actual differences may be lost in the uncertainties. One does not conclude that the failure diameters are the same, nor does one conclude that they are not.

Also note that, if the 40B/60 data from Table 8 are plotted in Figures 9, 10 and 11 (this was not done), excellent agreement with the other data occurs. Based on the Campbell-Engelke model of diameter effects, it would probably be appropriate to include those data in Figures 9, 10 and 11, since they would lie on the nonconcave portion of the curve described by Equation (6), i.e., the dashed line in Figure 9. A simple examination shows that these data do lie on that line.

At this point, we terminate discussion of the 40/60 and 40B/60 data in that nothing further can be contributed to real understanding of the detonation performance of HMX/emulsion mixtures.

SECTION 5
CONCLUSIONS

At the completion of the experimental program described in this report, it was clear that many additional experiments would be required to provide a complete description of the detonation performance of HMX/emulsion mixtures. Given that it was not possible to obtain good mixes for HMX loadings greater than 50 percent, the additional experiments needed are for detonation velocity-diameter data for mixtures below 20 percent HMX and for more refined data on failure diameter and velocity at failure for all mixtures. Schedule and funding constraints did not permit additional experiments. Nevertheless, it was possible to provide velocity-mixture-diameter data over a region sufficient to provide a definitive description of the behavior of HMX/emulsion mixtures over the range of 20 to 50 percent HMX and a qualitative description over the entire range of mixtures. The results of this research should be valuable in pointing the way for future research on the detonation performance of molecular/emulsion explosive systems.

The main conclusions of this research are summarized as follows:

(1) At a given diameter, an increase in HMX loading results in an increase in detonation velocity. As HMX loading increases, the failure diameter decreases and the detonation velocity at failure increases. The trend in velocity at failure was evident in the data but precise measurements of velocity at failure were not obtained. The qualitative behavior predicted in Figure 1 has been confirmed.

(2) The diameter effect on detonation velocity for HMX/emulsion mixtures is adequately described by the Campbell-Engelke model. This was clearly demonstrated for the 50/50 mixture and the trend of downward concavity on the D vs 1/d curve was observed for other mixtures.

(3) Addition of approximately 20 percent HMX to the emulsion results in a substantial increase in initiation sensitivity. This

observation is based on the premise (which is believed to be true for the HMX/emulsion mixtures) of an inverse relationship between failure diameter and initiation sensitivity. An interesting area of future research would be to investigate the combined effects of particle size and mass loading of a molecular explosive on initiation sensitivity and failure diameter.

(4) The particular emulsion formulation developed in this research exhibited (in most cases) remarkable physical stability. After preparation of the emulsion, HMX was added in a high shear mixing operation at room temperature, and the mixture was subjected to additional shear during preload and test article loading operations - also at room temperature. Samples of the pure emulsion have been observed for over one year with only slight clouding of the emulsion.

(5) A variety of physical properties of the HMX/emulsion mixtures were observed, depending on the HMX loading, HMX particle size and shear history. The four classes of properties observed were:

(a) Stiff grease - obtained for HMX loadings from 10 to 50 percent for coarse grade HMX.

(b) Noncohesive powder - obtained for mixtures of coarse grade HMX for loadings above 50 percent and for fine grade HMX at a loading of 50 percent.

(c) Hard - obtained for coarse grade HMX at a loading of 50 percent when subjected to high shear.

(d) Nontacky putty - obtained for the 40B/60 mixture.

The castable (hard) and putty-like consistencies have properties that make them of interest in a number of potential applications. Because the physical nature of the 50/50 cast mixture is unknown, its initiation sensitivity to shock, friction and spark effects should be thoroughly

characterized during the initial phase of any future research program involving that material.

(6) While no firm conclusions are made based on the 40B/60 and 40/60 data relative to the effects of HMX particle size on detonation performance, the downward concavity observed in the D versus 1/d curve demonstrates that the hot-spot mechanism controls propagation of detonation at small diameters; and thus it would be predicted that a decrease in particle size would result in a decrease in failure diameter as well, since for a given mass loading the number of initiation sites would increase in direct proportion to the inverse cube of the particle diameter.

REFERENCES

1. Campbell, A.W., Davis, W.C. and Travis, J.R., "Shock Initiation of Detonation in Liquid Explosives", Phys. Fluids 4, 498-510 (1961).

2. Campbell, A.W., Davis, W.C., Ramsay, J.B. and Travis, J.R., "Shock Initiation of Solid Explosives", Phys. Fluids 4, 511-521 (1961).

3. Johansson, C.H. and Persson, P.A., Detonics of High Explosives, Academic Press, London, England, 81-156 (1970).

4. Lee, J., "The Effect of Microballoon Size on Detonation Behavior of Emulsion Explosives", Masters Thesis, New Mexico Institute of Mining and Technology, Socorro, NM (1987).

5. Yoshida, M., Iida, M., Fujiwara, S., Kusakabe, M., and Shiino, K., "Detonation Behavior of Emulsion Explosives Containing Microballoons," Eighth Symposium (International) on Detonation, 171-177 (1985).

6. Hattori, K., Fukatsu, Y. and Sakai, H., "Effect of the Size of Glass Microballoons on the Detonation Velocity of Emulsion Explosives", J. Ind. Explos. Soc. Japan, 43, 295-309 (1982).

7. Oxley, J. and Griffith, G., private communication, May 1987.

8. Operating Instruction Manual, LeCroy Multichannel Digital Oscilloscope Model 6900-1, LeCroy Research Systems Corp., Spring Valley, NY.

9. Operating Instruction Manual, Model 770 Synchronized Sweeping Image Camera, Beckman & Whitley, San Carlos, CA (1963).

10. Mader, C.L., "Detonation Properties of Condensed Explosives Computed Using the Becker-Kistiakowsky-Wilson Equation-of-State", Los Alamos Scientific Laboratory Report No. LA-2900, June 17, 1963.

11. Private communication between B. Craig and J. Lee, July 1985.

12. Smith, L.C., "On Brisance, and a Plate-Denting Test for the Estimation of Detonation Pressure", Explosivstoffe, No. 5, 106 (1967).

13. Campbell, A.W. and Engelke, R., "The Diameter Effect in High Density Heterogenous Explosives," Sixth Symposium (International) on Detonation, ACR-221, 642-652 (1976).

APPENDIX

BALANCE

PROGRAM LISTING

```
10 '  PROGRAM IS "BALANCE". CALCULATES OXYGEN BALANCE
20 '  FOR EXPLOSIVES COMPOSED OF CARBON, HYDROGEN, OXYGEN,
30 '  NITROGEN, SODIUM AND ALUMINUM.  CALCULATIONS ARE BASED
40 '  ON REDUCTION OF ALL REACTANTS TO H20 AND CO2.
50 '
60 '  WRITTEN BY J. RENICK, AIR FORCE WEAPONS LABORATORY, 24 FEB 88.
70 '
80    DIM C(10),H(10),O(10),AL(10),N(10),NA(10),OB(10),X(10)
90    DIM A$(10)
100   MWC=12
110   MWH=1
120   MWN=14
130   MWO=16
140   MWAL=27
150   MWNA=23
160   INPUT "EXPLOSIVE NAME?";Z$
170   LPRINT Z$
180   LPRINT "  "
190   LPRINT "  "
200   INPUT "NUMBER OF REACTANTS =";NR
210   FOR I=1 TO NR STEP 1
220   INPUT "REACTANT NAME?";A$(I)
230   INPUT "CARBON=";C(I)
240   INPUT "HYDROGEN=";H(I)
250   INPUT "OXYGEN=";O(I)
260   INPUT "ALUMINUM=";AL(I)
270   INPUT "SODIUM=";NA(I)
280   INPUT "NITROGEN=";N(I)
290   MWT=C(I)*MWC+H(I)*MWH+N(I)*MWN+O(I)*MWO+AL(I)*MWAL+NA(I)*MWNA
300   OB(I)=-(2*C(I)+H(I)/2+1.5*AL(I)-O(I))*(MWO/MWT)
310   NEXT I
320   LPRINT "  "
330   LPRINT "  "
340   LPRINT "REACTANT/C/H/N/O/AL/NA/OXYGEN BALANCE"
350   LPRINT "  "
360   FOR I=1 TO NR STEP 1
370   LPRINT A$(I);C(I);H(I);N(I);O(I);AL(I);NA(I);OB(I)
380   NEXT I
390   FOR I=1 TO NR STEP 1
400   PRINT "  "
410   PRINT A$(I)
420   INPUT "MASS FRACTION =";X(I)
430   NEXT I
440   OXB=0
450   FOR I=1 TO NR STEP 1
460   OXB=OXB + X(I)*OB(I)
470   NEXT I
480   LPRINT "  "
```

HMX

HMX EMULSION MIXTURES
USE EMULSIONS
HMX
MIXTURES

MIXTURES OF HMX
USE HMX
MIXTURES

WATER
USE WATER

PHRASES NOT FOUND DURING LEXICAL DICTIONARY MATCH PROCESS

10 TO 50

HMX

HMX EMULSION MIXTURES
  USE EMULSIONS
      HMX
      MIXTURES

MIXTURES OF HMX
  USE HMX
      MIXTURES

WATER
  USE WATER

PHRASES NOT FOUND DURING LEXICAL DICTIONARY MATCH PROCESS

10 TO 50